Acta Mechanica Slovaca **29 (1): 28 - 35,** March **2025**
https://doi.org/10.21496/ams.2025.009

Acta Mechanica Slovaca
ISSN 1335-2393
www.actamechanica.sk

Coupling DRNN with Numerical Simulations for the Thermal Performance Analysis of a Shell-and-Tube Heat Exchanger Using Cu/Water Nanofluid

Bouhelal Guendouz [1,2], Hamidou Benzenine [1,2,*], Mohammed Beldjilali [3,4], Kaddour Bahram [2,5] and Rachid Saim [1,2]

[1] Laboratory of Energetic and Applied Thermal, ETAP, Department of Mechanical Engineering, Faculty of Technology,B.P 230, University of Tlemcen, 13000, Algeria
[2] University of Ain Témouchent, Belhadj Bouchaib, Department of Mechanical Engineering, PO Box 284,46000, Algeria
[3] University of Ain Témouchent, Belhadj Bouchaib, Department of Material Sciences, PO Box 284,46000, Algeria
[4] Laboratory of Applied Chemistry (LAC), University of Ain Temouchent, Algeria
[5] Laboratory of Materials and Reactive Systems LMSR, Department of Mechanical Engineering, University Djilali Liabes, BP 89, Cité Ben M'hidi, Sidi bel Abbes, 22000, Algeria

Abstract: This study investigates the thermal performance of a shell-and-tube heat exchanger, enhanced by using a Cu–water nanofluid on the shell side. A combined experimental and numerical approach was used to assess the effects of varying nanoparticle concentrations (2% to 6%) and cold-side flow rates (0.047 to 4 l/min). At 6% concentration, results showed a temperature increase of up to 7 °C on the shell side, a 12% improvement in thermal efficiency, and a global heat transfer coefficient reaching 8516.87 W, compared to pure water. Additionally, a deep recurrent neural network (DRNN) was implemented to predict key performance indicators: thermal efficiency, heat transfer coefficient, and outlet temperature on the shell side. The model, trained on various thermal parameters, demonstrated excellent predictive accuracy (R^2 = 0.997, 0.998, and 0.984) with low RMSE, MAE, and MSE values.

Keywords: Nanofluids, STHE (Shell-and-Tube Heat Exchanger), CFD Numerical Simulation, Global Heat Transfer Coefficient, Copper.

1. Introduction

Heat transfer enhancement processes are one of the key areas of continuous research due to their importance in energy-saving applications across various fields. One of the most crucial devices used in thermal energy conservation is the heat exchanger, particularly shell-and-tube heat exchangers (STHE). More than 35% to 40% of the heat exchangers used in global heat transfer processes are shell-and-tube heat exchangers. This is primarily due to their robust structural design, ease of maintenance, and the potential for upgrades [1].

However, their thermal efficiency is often limited by the inherently low thermal properties of conventional heat transfer fluids such as water, ethylene glycol, and oil. Nanofluids have emerged as an innovative solution to enhance the thermal performance of heat exchangers.

Nanofluids are dilute liquid suspensions of nanoparticles, with at least one critical dimension smaller than 100 nm, stably and uniformly dispersed in a base fluid to enhance its thermal properties, particularly thermal conductivity.

Thanks to the high thermal conductivity of nanoparticles, the thermophysical properties of the heat transfer fluid are improved. Consequently, the resulting

*** Corresponding author:** Hamidou Benzenine, ***E-mail address:*** *hamidou.benzenine@univ-temouchent.edu.dz*

nanofluid optimizes heat transfer, thereby reducing equipment size, energy costs, and pressure losses.

In this context, numerous studies have focused on the use of nanofluids to enhance the performance of shell-and-tube heat exchangers. One of the earliest studies was conducted by P.A.D. Cruz et al. [2], who performed a CFD numerical analysis of turbulent CuO-W nanofluid (NF) flow on the shell side of an STHE. They found that a 0.1% concentration could increase heat transfer by up to 12%. Performance indices above 1 were obtained for a volume fraction below 0.25%.

M. Bahiraei et al. [3] numerically compared the effect of different shapes of boehmite nanoparticles in a water/ethylene glycol (50/50) mixture on the tube side of an STHE. They concluded that platelet-shaped nanoparticles resulted in the highest overall heat transfer coefficient, while oblate spheroid (OS) nanoparticles exhibited the lowest pressure drop and the highest efficiency. The evaluation of irreversibility characteristics for the same problem was conducted in a subsequent study [4], where they observed a decrease in thermal entropy generation (TEG) and the Bejan number (Be), along with an increase in frictional entropy generation (FEG) as the Reynolds number (Re) increased.

N. Kumar et al. [5] experimentally investigated heat transfer on the tube side of an STHE using Fe_2O_3-W and Fe_2O_3-EG nanofluids. They demonstrated that the overall heat transfer coefficient (U) and the Nusselt number (Nu) improved with increasing concentration, temperature, and Reynolds number (Re). However, an increase in Re also led to a greater pressure drop (Δp).

The thermo-hydraulic behaviour of turbulent nanofluid flow in the cubic shell of an STHE was numerically studied by A.K. Kareem et al. [6]. This study highlighted that SiO_2-W, TiO_2-W, CuO-W, and Al_2O_3-W nanofluids exhibited significant heat transfer improvements compared to pure water.

V. Ghazanfari et al. [7] used CFD to analyse the efficiency of an STHE fed by a turbulent nanofluid flow on the shell side. They found that using Cu nanoparticles at 0.1% and Al_2O_3 nanoparticles at 0.15% enhanced heat transfer by 1.04 and 1.12 times, respectively. Additionally, the maximum pressure drop for Cu, CuO, TiO_2, and Al_2O_3 was approximately 30%, 26%, 22%, and 19%, respectively, compared to water.

The enhancement of thermal performance on the tube side of an STHE using three other types of nanofluids was investigated by I.M. Shahrul et al. [8]. Improvements of approximately 35%, 26%, and 12% in the overall heat transfer coefficient (U); 50%, 15%, and 9% in the heat transfer coefficient; and 51%, 32%, and 26% in actual heat transfer were observed for ZnO-W, Al_2O_3-W, and SiO_2-W nanofluids, respectively, compared to water.A.M. Hassaan [9] experimentally studied the efficiency of using MWCNT (multi-walled carbon nanotube) nanofluid based on water flowing through the tubes of an STHE. An optimal nanofluid concentration of 2% was determined, resulting in improvements of 76.4%, 55.6%, and 37.6% in the overall heat transfer coefficient (U), Nusselt number (Nu), and efficiency, respectively, compared to distilled water.

Another experimental investigation on the thermal behaviour of γ-Al_2O_3-W and TiO_2-W nanofluids flowing through the tube bundle side of an STHE was conducted by B. Farajollahi et al. [10]. The results indicated that both nanofluids have different optimal concentrations at which heat transfer characteristics are maximized. TiO_2 nanoparticles exhibited a lower optimal concentration. MWCNT nanofluid was also analysed numerically in a hybrid formulation in the study by A. Brakna et al. [11]. This investigation focused on the influence of different hybrid nanofluids with varying nanoparticle percentages in an oil-based medium, specifically Al_2O_3-MWCNT and MgO-MWCNT, with different fractions and flow rates, on heat transfer rates in a double-pipe heat exchanger. The results highlighted the advantage of using Al_2O_3-MWCNT/oil nanofluid at a (25:75) ratio. Its use as the hot fluid in the inner tube maximized heat transfer and improved the performance of the studied heat exchanger. A.A. Lokhande et al. [12] numerically observed that the overall heat transfer coefficient improved by a factor of 1.27 to 1.66, and the heat transfer rate increased by 1.2 to 1.66 for volume concentrations ranging from 0.01% to 0.02%, respectively, compared to water in a turbulent CuO-W flow inside the tubes of an STHE. K.Y. Leong et al. [13] modeled the heat recovery phenomenon in an STHE, where combustion gases flowed through the shell while Cu-W and Cu-EG nanofluids circulated through the tubes. They reported that approximately 16.9% and 9.5% improvements in the heat transfer coefficient (h) and overall heat transfer coefficient (U), respectively, were recorded for EG

at a 1% volume fraction compared to the base fluid. K. Somasekhar et al. [14] numerically studied heat transfer enhancement in a multi-pass STHE, where an Al_2O_3-W nanofluid flowed inside its tubes. For a Peclet number of 60,000, they found that the overall heat transfer coefficient (U) increased by 0.28% to 2.6%, and the Nusselt number (Nu) improved by 0.55% to 7.54% compared to water for nanofluid concentrations ranging from 0.3% to 2%, respectively. L. Godson et al. [15] experimentally investigated the thermal characteristics of turbulent Ag-W nanofluid flow on the tube side of an STHE. They observed that the increase in the heat transfer coefficient for concentrations of 0.01%, 0.03%, and 0.04% was 9.2%, 10.87%, and 12.4%, respectively. Maximum recorded values for the heat transfer coefficient, efficiency, and pressure drop were 12.4%, 6.14%, and 16.22%, respectively, at Re = 25,000 and a nanofluid concentration of 0.04%, compared to water.

This study is based on a numerical analysis of the impact of various nanofluid concentrations and inlet flow rates on the thermal performance of a shell-and-tube heat exchanger (STHE). An experimental setup with the same configuration was conducted in parallel to validate the numerical findings.

A deep recurrent neural network (DRNN) was also employed to predict key performance indicators: thermal efficiency, heat transfer coefficient, and shell-side outlet temperature. The network architecture was carefully optimized to ensure accurate estimation of the exchanger's thermal behaviour.

2. Geometric Configuration of the STHE and Experimental Setup

The geometric specifications of the heat exchanger studied in this work are illustrated in the graphical representation in Figure 1. It is a single-pass shell-and-tube heat exchanger containing seven stainless steel tubes with inner and outer diameters of 4 mm and 6 mm, respectively. The tubes, which have a length of 180 mm, are arranged in a triangular pattern with a pitch of 15 mm. The ends of the tube bundle are connected by a distribution box at the inlet and a collection box at the outlet.

The shell has a cylindrical shape with an inner and outer diameter ranging from 50 mm to 60 mm. It is equipped with three segmented baffles, each 1 mm thick, distributed with a spacing of 44.25 mm.

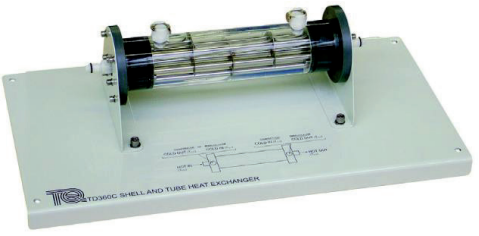

Figure 1: Geometric Configuration of the Studied Heat Exchanger.

Each baffle contains a window with a height of 20 mm. The inlet and outlet diameters for the tube-side fluid are 12 mm, while the inlet and outlet diameters for the shell-side fluid are 10 mm.

The experimental setup consists of two separate fluid loops: one hot and one cold. Each loop includes a storage tank, circulation pump, thermocouples at inlet and outlet points, a flowmeter, and a flow control valve. Key measurements include inlet/outlet temperatures and volumetric flow rates.

The cold fluid flows through the shell via Pump 1, while the hot fluid passes through the tubes via Pump 2. Four type-K thermocouples monitor temperatures at both inlets and outlets. A counterflow configuration was selected to enhance thermal exchange efficiency between the two fluids.

3. Numerical Simulation

In the same context, a numerical simulation was performed using Ansys Fluent to study the heat transfer performance of our heat exchanger. In this case, a nanofluid was used as the cold fluid circulating in the shell, while hot water flowed through the tubes, maintaining a counterflow configuration.

3.1. Governing Equations

In this study, the Reynolds-Averaged Navier-Stokes (RANS) equations, employing the realizable k-ε model with enhanced wall treatment, are used. The governing equations for continuity, momentum, and energy in a steady-state, three-dimensional flow are expressed as follows:

» *Continuity equation:*

$$\frac{\partial u_i}{\partial x_i} = 0 \qquad (1)$$

» *Momentum equation:*

$$\frac{\partial u_i u_j}{\partial x_i} = \frac{1}{\rho}.\frac{\partial p}{\partial x_i} + \frac{\partial}{\partial x_i}.\left[(\nu + \nu_t).\left(\frac{\partial u_j}{\partial x_i} + \frac{\partial u_i}{\partial x_j} \right) \right] \qquad (2)$$

» *Energy equation:*

$$\frac{\partial u_i.T}{\partial x_i} = \frac{\partial}{\partial x_i}.\left[\left(\frac{\nu}{Pr} + \frac{\nu_t}{Pr_t}\right).\frac{\partial T}{\partial x_i}\right] \quad (3)$$

Numerical simulations were carried out using the Ansys FLUENT computational code. The pressure-based solver and the SIMPLE coupling algorithm were adopted. For discretization schemes, second-order was selected for pressure, while the second-order upwind scheme was used for momentum, turbulent kinetic energy, dissipation rate, and energy equations. The convergence criteria, which were integrated norms within ANSYS, were used in this study. These convergence criteria are based on residuals with a minimum order of 10^{-3}.

3.2. Simplifying Assumptions

The problem is mathematically modeled based on the following assumptions:

– *The flow is considered continuous, Newtonian, and incompressible.*

– *Fluid leakage, gravity, and viscous thermal effects are neglected.*

– *A single-phase approach is applied in the nanofluid modeling, assuming that nanoparticles are perfectly homogenized in the base fluid.*

– *Heat transfer is assumed to occur only through conduction and convection; all forms of radiation are considered negligible.*

– *Particle mechanisms and interactions such as aggregation, sedimentation, fouling effects, and other drawbacks associated with nanofluids are not considered in this study.*

3.3. Thermophysical Properties of Nanofluids

In this work, a Cu/water nanofluid is employed, with copper nanoparticles dispersed in water at volume fractions (φ) ranging from 2% to 6%. The nanofluid's thermophysical properties—density, specific heat capacity, thermal conductivity, and viscosity—are computed using classical models, assuming constant properties for water and copper (see Table 1).

» *Density*

$$\rho_{nf} = (1-\varphi).\rho_{bf} + \varphi.\rho_{np} \quad (4)$$

» *Specific heat capacity*

$$(\rho.C_p)_{nf} = (1-\varphi).(\rho.C_p)_{bf} + \varphi.(\rho.C_p)_{np} \quad (5)$$

» *Dynamic viscosity (Brinkman model)*

$$\mu_{nf} = \mu_{bf} / (1-\varphi)^{2,5} \quad (6)$$

» *Thermal conductivity (Maxwell model)*

$$\lambda_{nf} = \lambda_{bf}.\frac{\lambda_{np} + 2.\lambda_{bf} + 2.\varphi.(\lambda_{np} - \lambda_{bf})}{\lambda_{np} + 2.\lambda_{bf} - 2.\varphi.(\lambda_{np} - \lambda_{bf})} \quad (7)$$

Where: **φ** is the nanop article volume fraction; Subscripts **bf, np,** and **nf** refer to the base fluid, nanoparticle, and nanofluid, respectively.

Table 1: Thermophysical Properties of Water and Copper Nanoparticles

Properties	Water	Copper
Cp (J/kg.K)	4179	385
ρ (kg/m3)	998	8933
λ (W/m.K)	0,613	395
M (Pa.s)	0,001	---

3.4. Boundary Conditions

– *No-slip boundary condition is assumed for all walls (the velocity field at the wall is zero).*

– *The shell-side wall is assumed to be perfectly insulated by assigning it a zero heat flux.*

– *At each inlet (tubes and shell), the velocity and temperature fields are assumed to be uniform and constant.*

– *Atmospheric pressure is applied at all outlets of the system (tubes and shell).*

– *Internal interfaces are thermally coupled in a solid-liquid interaction.*

4. Method deep neural network (DNN)

In this study, the technique of artificial intelligence deep neural networks was utilized to analyse the influence of various input features on the thermal efficiency Ec, Heat transfer coefficient Kc and the outlet temperature of the fluid on the shell side (Tout_calandreT) efficiency. The dataset comprised key variables, including shell and tube inlet velocities and temperatures, mean logarithmic temperature difference and shell and tube heat flux exchanged (U-In_Calandre, U-In_Tube, T-In_Calandre, T-In_Tube, DTLM, NET-calandre-total-heattransfer and NET-tube-total-heat-transfer) as inputs with others as the output. The workflow of this research was structured into four distinct stages: 1) data collection, 2) data pre-processing, 3) model training, and 4) testing using a deep neural network architecture.

5. Mesh Strategy and Independence Study

A structured and uniform mesh was employed, with local refinement around the tube surfaces to accurately capture temperature gradients. Several grid density tests were conducted to ensure mesh independence of the simulation results. Figure 2 presents the variation of the STHE outlet

temperatures as a function of the number of mesh cells.

Based on the sensitivity analysis, the results began to stabilize beyond 1,846,683 cells. Consequently, a final mesh with 2,330,332 elements was selected for the numerical simulations, ensuring both accuracy and reliability of the computational model.

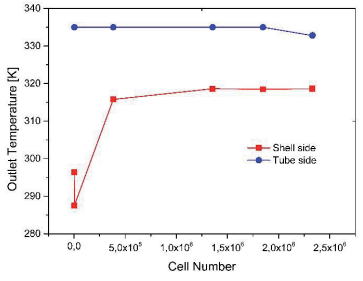

Figure 2: Variation of the STHE exchanger outlet temperatures as a function of the number of mesh cells.

6. Numerical Validation Against Experimental Results

The numerical simulation results were validated by comparing them with experimental data using the same STHE configuration and water as the working fluid on both shell and tube sides.

For this comparison, the inlet temperatures were set at 333 K for the hot fluid and 300 K for the cold fluid. The hot fluid flow rate in the tubes was kept constant at 2.5 L/min, while the cold fluid flow rate in the shell varied between 0.5 and 4 L/min.

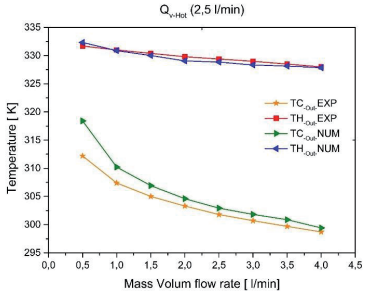

Figure 3: Comparison Between Numerical and Experimental Results

Figure 3 shows the variation of outlet temperatures for both fluids as a function of the shell-side flow rate. As shown, a good agreement is observed between numerical and experimental results, confirming the accuracy of the simulation procedure. Furthermore, the maximum relative error remains below 1.95% on the shell side and 0.22% on the tube side of the heat exchanger, demonstrating the reliability and robustness of the numerical model.

7. Results and Interpretations

In this study, the heat transfer performance of Cu-W nanofluids in a three-dimensional shell-and-tube heat exchanger (STHE) is analysed using the finite volume method. The effects of the nanofluid's volumetric concentration (ranging from 2% to 6%) and volumetric flow rate (0.047 to 4 L/min) on flow behaviour and heat transfer are investigated.

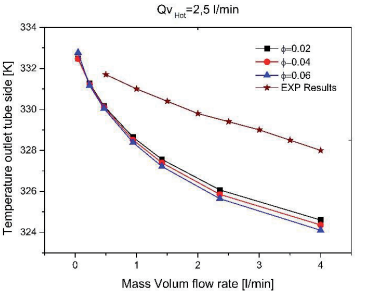

Figure 4: Evolution of Hot Water Outlet Temperature (Tube Side) as a Function of Nanofluid Volumetric Flow Rate

Figure 4 illustrates the evolution of the hot water temperature as a function of the nanofluid volumetric flow rate for three selected volumetric concentrations. These results are also compared with experimental data in which pure water without nanoparticles was the only fluid flowing through the both sides of the heat exchanger.

It is observed that the hot fluid temperature gradually decreases with increasing nanofluid flow rate in the shell. Additionally, this temperature increases as the nanoparticle concentration decreases, indicating that the presence of nanoparticles enhances heat transfer by absorbing more energy.

The temperature difference between the hot water interacting with the nanofluid on the shell side and the hot water in the tube (experimental results) varies as follows:

– *(1.54, 1.59, 1.66 K) for concentrations of 0.02, 0.04, and 0.06 at a flow rate of 0.047 l/min.*

– *(3.40, 3.64, 3.90 K) for the same concentrations at a higher flow rate of 4 l/min.*

These results demonstrate that using nanofluids in the shell enhances heat exchange compared to using water alone. However, it is noted that the water in the tube retains a higher temperature, meaning it holds more thermal energy instead of effectively transferring it to the nanofluid. A portion

of this energy could be dissipated externally, leading to thermal losses in the system.

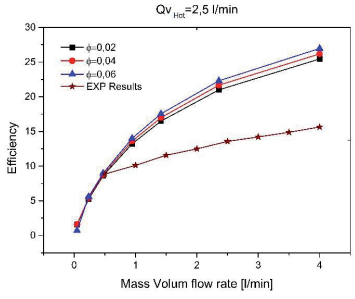

Figure 5: Relationship Between the Thermal Efficiency of the STHE and the Cold Fluid Volumetric Flow Rate for Different Nanofluid Concentrations

Figure 5 illustrates the relationship between the thermal efficiency of the STHE and the cold fluid volumetric flow rate, considering different nanofluid concentrations. These results are also compared with the experimental data obtained in this study.

It is observed that the heat exchanger's efficiency increases with the rise in the cold fluid volumetric flow rate, regardless of the case studied. However, the increase in nanoparticle volume fraction further enhances this efficiency.

The numerical results demonstrate an improvement in the thermal efficiency of the STHE compared to the experimental data, thanks to the use of the nanofluid and the increase in its flow rate.

The use of the Cu-water nanofluid resulted in an efficiency gain ranging from:

– *0.26% to 0.11% for a 2% concentration.*

– *9.81% to 11.33% for a 6% concentration, compared to the efficiency obtained experimentally with water alone.*

These results confirm that the integration of nanoparticles significantly improves heat transfer in the STHE, especially when their concentration and the cold fluid flow rate increase.

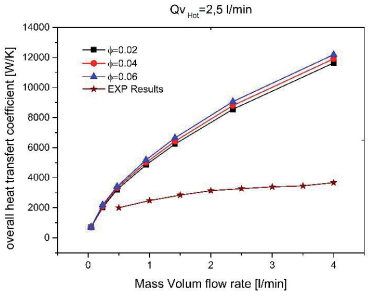

Figure 6: Evolution of the Overall Heat Transfer Coefficient as a Function of the Nanofluid Volumetric Flow Rate in the Shell Side.

Figure 6 highlights an increase in the overall heat transfer coefficient with the rise in the nanofluid volumetric flow rate circulating in the shell side of the heat exchanger.

A slight difference is observed between the three curves corresponding to different nanofluid concentrations, with this difference becoming more pronounced as the cold fluid flow rate increases.

The experimental values follow the same trend but with a lower slope compared to the numerical results. This suggests that the numerical simulation tends to slightly overestimate the improvement in heat transfer.

The results indicate that the overall heat transfer coefficient obtained with the Cu-W nanofluid is significantly higher than with water alone. The values obtained are in the range of:

– *1205.90 W to 1409.66 W for a flow rate of 0.047 l/min.*

– *7962.79 W to 8516.87 W for a flow rate of 4 l/min.*

These findings confirm that the addition of nanoparticles significantly enhances heat transfer, making the heat exchanger more efficient, particularly at high cold fluid flow rates.

Figure 7 (A, B, and C) illustrates the performance of the Deep Recurrent Neural Network (DRNN) algorithm during both the training and testing phases over multiple epochs.

The results obtained from the models exhibit high R^2 values, demonstrating strong predictive accuracy for:

– *Thermal efficiency (Ec)*

– *Heat transfer coefficient (Kf)*

– *Outlet temperature of the fluid on the shell side (T-out-calandre)*

The corresponding R^2 values are **0.997**, **0.998**, and **0.984** for **Ec, Kf,** and **T-out-Calandre**, respectively.

These high R^2 values indicate an excellent agreement between the experimental results and the predicted values, reinforcing the reliability and precision of the DRNN model.

Figure 7 shows the statistical metrics (RMSE, MAE, MSE, and R^2) were used to assess the predictive performance of the model for three parameters: Ec, Kf, and T-out calandre. The model exhibited excellent performance, achieving high R^2 values of 0.996, 0.936, and 0.99 for Ec, Kf, and T-out calandre, respectively, indicating a strong alignment between predicted and actual values. Low RMSE and MSE values further confirm the model's accuracy and precision.

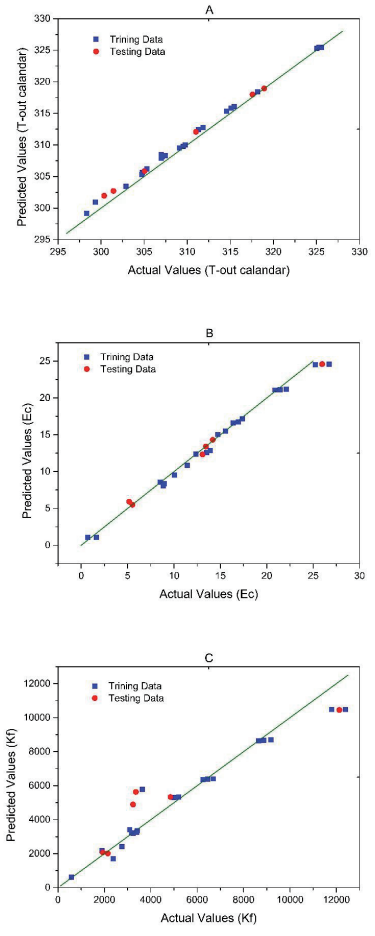

Figure 7: Training and Testing of DRNN model algorithm for; A: the thermal efficiency, B: Heat transfer coefficient and C: the outlet temperature of the fluid on the shell side.

Table 2: Statistical Evaluation of Model Accuracy for Ec, T-out-Calandre, and Kf

Statistics of Model	Ec	T-out-Calandre	Kf
RMSE	0.401	1.85	74.99
MAE	0.307	1.68	50.53
MSE	0.16	3.43	5624
R2	0.996	0.986	0.99

8. Conclusion

A numerical study using the Finite Volume Method in ANSYS Fluent was conducted to assess the thermal performance and efficiency of a shell-and-tube heat exchanger (STHE). The impact of using a Cu/water nanofluid on the shell side, with volumetric concentrations ranging from 2% to 6% and varying flow rates (0.047 to 4 L/min), was evaluated. Additionally, experimental tests on the same heat exchanger, using only water on both the shell and tube sides, were carried out to validate and compare results in terms of outlet temperatures, efficiency, and overall heat transfer coefficient.

The results reveal the following conclusions:

– The use of Cu/water nanofluid on the shell side significantly enhances heat transfer compared to pure water, regardless of the nanofluid concentration.

– Increasing the nanofluid concentration to 6% improves the heat exchanger's thermal performance, leading to:

- *» A temperature rise of up to 7°C on the shell side and 4°C on the tube side.*
- *» A 12% improvement in thermal efficiency.*
- *» A rise in the overall heat transfer coefficient, from 1,409.66 W to 8,516.87 W, depending on the flow rate (0.047–4 L/min), compared to experimental results with water.*

The study investigates the application of a Deep Recurrent Neural Network (DRNN) for predicting thermal efficiency, heat transfer coefficient, and outlet fluid temperature on the shell side, emphasizing its practical applicability. The predictive performance of the DRNN model was rigorously validated against experimental data to ensure accuracy and reliability. The results indicate high R^2 values, demonstrating strong predictive performance: Thermal efficiency (Ec): R^2 = 0.997, Heat transfer coefficient (Kf): R^2 = 0.998, and Outlet temperature on the shell side (T-out-Calandre): R^2 = 0.984.

These high R^2 values confirm a strong correlation between experimental data and model predictions, highlighting the DRNN model's reliability and precision in capturing the underlying thermal characteristics of the system.

References

[1] I. Master Bashir, S. Chunangad Krishnan, and Pushpanathan Venkateswaran, (2003) Fouling Mitigation Using Helixchanger Heat Exchangers. in Engineering Conferences International, 1-6.

[2] E. J. E. Yamat, J. P. E. Nuqui, A. N. Soriano P. A. D. Cruz (2022) Computational Fluid Dynamics (CFD) analysis of the heat transfer and fluid flow of copper (II) oxide-water nanofluid in a shell and tube heat exchanger, Digital Chemical Engineering, 1-14.

[3] M.Naseri, A.Monavari M. Bahiraei(2022) Thermal-hydraulic performance of a nanofluid in a shell-and-tube heat exchanger equipped with new trapezoidal inclined baffles:

Nanoparticle shape effect, Powder Technology, 348-359,.

[4] M.Bahiraei and A.Monavari (2022) Irreversibility characteristics of a mini shell and tube heat exchanger operating with a nanofluid considering effects of fins and nanoparticle shape Powder Technology 1-11.

[5] N.Kumar and S.S. Sonawane (2016) Experimental study of Fe2O3/water and Fe2O3/ethylene glycol nanofluid heat transfer enhancement in a shell and tube heat exchanger. International Communications in Heat and Mass Transfer, no. 78 277-284.

[6] A.K.Kareem, A.H.Alabbasi, and A.M.Mohsen (2024) Simulation study of heat transfer behaviour of turbulent two-phase flow in a 3D cubic shell and tube heat exchanger using water and different nanofluids. Results in Engineering, no. 24 1-13 .

[7] V.Ghazanfari, A.Taheri, Y.Amini, and F.Mansourzade (2024) Enhancing heat transfer in a heat exchanger: CFD study of twisted tube and nanofluid (Al2O3, Cu, CuO, and TiO2) effects. Case Studies in Thermal Engineering, no. 53 1-18.

[8] I.M. Shahrul, I.M. Mahbubul, R. Saidur, and M.F.M. Sabri (2016) . International Journal of Heat and Mass Transfer, no. 97 547-558.

[9] A.M.Hassaan, (2022)An investigation for the performance of the using of nanofluids in shell and tube heat exchanger. International Journal of Thermal Sciences, no. 177 1-8.

[10] B.Farajollahi, S.G.Etemad, and M.Hojjat, (2010) Heat transfer of nanofluids in a shell and tube heat exchanger International Journal of Heat and Mass Transfer, no. 53 12-17.

[11] D.A.BRAKNA and H.BENZENINE, (2024) Computational Analysis of Hybrid Nanofluid Flow in a Double-Tube Heat Exchanger: A Numerical Study Journal of Applied and Computational Mechanics 1-9.

[12] A.A.Lokhande, D.R.Waghole, and S.A.Dayane, (2023) Heat transfer augmentation in shell and tube heat exchangers using copper oxide nanofluid with modified geometry: A numerical investigationMaterials Today: Proceedings, no. 72 1240-1245.

[13] K.Y. Leong, R.Saidur, T.M.I.Mahlia, and Y.H.Yau, (2012) Modeling of shell and tube heat recovery exchanger operated with nanofluid based coolants International Journal of Heat and Mass Transfer, no. 55 808-816.

[14] K.Somasekhar et al., (2018) A CFD Investigation of Heat Transfer Enhancement of Shell and Tube Heat Exchanger Using Al2o3-Water Nanofluid Materials Today: Proceedings , no. 5 1057-1052.

[15] L.Godson, K.Deepak, C.Enoch, B.Jefferson, and B.Raja, (2014) Heat transfer characteristics of silver/water nanofluids in a shell and tube heat exchanger, Archives of Civil and Mechanical Engineering, no. 14 489-496.

[16] M.Gholami et al., (2020) Natural convection heat transfer enhancement of different nanofluids by adding dimple fins on a vertical channel wall, Chinese Journal of Chemical Engineering, no. 28 643-659 .